Endoluminal Gingival Fibroblast Transfer Reduces the Size of Rabbit Carotid Aneurisms via Elastin Repair

Eric Durand, Benjamin Fournier, Ludovic Couty, Mathilde Lemitre, Paul Achouh, Pierre Julia, Ludovic Trinquart, Jean Noel Fabiani, Sylvie Seguier, Bruno Gogly, Bernard Coulomb, Antoine Lafont

Objective—Matrix metalloproteinase-9 is considered to play a pivotal role in aneurismal formation. We showed that gingival fibroblasts (GF) in vitro reduced matrix metalloproteinase-9 activity via increased secretion of tissue inhibitor of metalloproteinase 1. We aimed to evaluate in vivo the efficacy of GF transplantation to reduce aneurism development in a rabbit model.

Methods and Results—Seventy rabbit carotid aneurisms were induced by elastase infusion. Four weeks later, GF, dermal fibroblast, or culture medium (DMEM) were infused into established aneurisms. Viable GF were abundantly detected in the transplanted arteries 3 months after seeding. GF engraftment resulted in a significant reduction of carotid aneurisms (decrease of 23.3% [$P<0.001$] and 17.6% [$P=0.01$] of vessel diameter in GF-treated arteries, 1 and 3 months after cell therapy, respectively), whereas vessel diameter of control DMEM and dermal fibroblast–treated arteries increased. GF inhibited matrix metalloproteinase-9 activity by tissue inhibitor of metalloproteinase 1 overexpression and matrix metalloproteinase-9/tissue inhibitor of metalloproteinase 1 complex formation, induced elastin repair, and increased elastin density in the media compared with DMEM-treated arteries (38.2 versus 18.0%; $P=0.02$). Elastin network GF-induced repair was inhibited by tissue inhibitor of metalloproteinase 1 blocking peptide.

Conclusion—Our results demonstrate that GF transplantation results in significant aneurism reduction and elastin repair. This strategy may be attractive because GF are accessible and remain viable within the grafted tissue. **(*Arterioscler Thromb Vasc Biol.* 2012;32:1892-1901.)**

Key Words: aneurism ■ cell therapy ■ elastin ■ fibroblasts ■ metalloproteinase

Abdominal aortic aneurism (AAA) is an increasingly frequent disease characterized by elastin and collagen destruction, smooth muscle cell apoptosis, and infiltration of inflammatory cells.[1–3] Matrix metalloproteinase-9 (MMP-9) is abundantly expressed in AAA and plays a pivotal role in aneurismal formation.[4,5] MMP-9 deficiency protects apolipoprotein E–deficient mice against atherosclerotic media destruction and ectasia.[6]

Presently, surgical and percutaneous endovascular AAA treatments do not specifically target the mechanisms of the AAA development.[1] In animal models, therapeutic strategies decreasing MMP-9 secretion in the aortic wall showed protection against AAA development. Overexpression of MMP-9 inhibitors (plasminogen activator inhibitor 1 and tissue inhibitor of metalloproteinase 1 [TIMP-1]) stabilizes arterial aneurisms in rat models.[7,8] However, these strategies require gene transfer, rendering this approach less applicable in human.[7–10] Endovascular transplantation of vascular smooth muscle cells (VSMC) has also been evaluated in rat models.[11] This treatment stabilizes the development of experimental aneurisms, but VSMC undergo apoptosis in human aneurismal lesions.[3,11] Moreover, autologous VSMC therapy is clinically inappropriate because it is not readily accessible in the perspective of autologous cell transfer.

We propose a novel cell therapy strategy based on a clinical observation: healing is known to be highly variable among different organs within the same human adult. The artery wall undergoes pathological postinjury remodeling, leading ultimately to stenosis or aneurism. Although gingiva is submitted to continuous and various injuries (mechanical, chemical, thermal, and infectious), it undergoes embryo-like repair (ie, without scar and fibrosis).[12,13] We recently showed in vitro and ex vivo that gingival fibroblasts (GF) dramatically reduced the aortic activity of MMP-9 related to increased TIMP-1 secretion, resulting in elastin preservation from degradation.[14] To further evaluate the concept of transfer of repair efficiency from 1 organ (gingiva) to compensate for the deficiency of another (artery), we aimed to evaluate in vivo the feasibility and efficacy of GF in established rabbit carotid aneurisms with a particular attention to the persistence and viability of transplanted GF in the arterial wall. To reinforce the relevance of our observations in animals, we also evaluated the effect of GF ex vivo on pathological human AAA samples collected from surgery.

Received on: October 5, 2011; final version accepted on: April 30, 2012.

From the Université Paris Descartes, INSERM, Assistance Publique-Hôpitaux de Paris, Laboratoire de Recherche Bio-Chirurgicale Fondation Alain Carpentier (E.D., B.F., L.C., M.L., P.A., P.J., L.T., J.N.F., S.S., B.G., B.C., A.L.); INSERM UMR 970, PARCC, European Georges Pompidou Hospital (E.D., B.F., L.C., M.L., P.A., P.J., J.N.F., S.S., B.G., B.C., A.L.); and Unité de Recherche Clinique (L.T.), Paris, France.

The online-only Data Supplement is available with this article at http://atvb.ahajournals.org/lookup/suppl/doi:10.1161/ATVBAHA.112.251439/-/DC1.

Correspondence to Eric Durand, INSERM U970, PARCC, 56 rue Leblanc, 75537 Paris cedex 15, France. E-mail eric.durand@egp.aphp.fr

Methods

GF and Dermal Fibroblast Cultures

Rabbit GF and dermal fibroblast (DF) cell cultures were obtained from New Zealand rabbit gingival and dermal explants, as previously described in DMEM (Life Technologies, Saint-Aubin, France) completed with 10% fetal bovine serum (Lonza, Basel, Switzerland).[14] In additional experiments (n=15), we used human GF for cell detection within the transplanted arteries using specific human antibodies (see below), because there is no specific marker of GF available at present. Human GF cultures were obtained from 3 healthy patients who gave their informed consent. Cultures were performed as previously described.[14] Each therapy consisted of 1 000 000 allogenic fibroblast suspensions in 1-mL serum-free DMEM (GF- or DF-treated arteries). Serum-free DMEM without cells (1 mL) was used as a control.

In Vivo Rabbit Experiments

The study design is summarized in File I in the online-only Data Supplement. The investigations conform to the *Guide for the Care and Use of Laboratory Animals* (National Institutes of Health Publication No. 85-23, revised 1996) and were in accordance with institutional guidelines.

We used a model of fusiform aneurism in rabbit carotid arteries induced by intraluminal infusion of elastase (n=70), as previously described.[15] Four weeks later, maximal external carotid diameter was measured using an electronic caliper. In fibroblast-treated arteries, GF or DF were injected into the lumen of clamped artery and were allowed to adhere during 15-minute contact. In control arteries, serum-free DMEM alone was similarly injected. Animals were euthanized by a lethal injection of pentobarbital 3 days and 1, 2, 3, 4, or 12 weeks after cell transplantation. Before euthanizing, maximal external carotid diameter was measured. Carotid arteries were retrieved and cut into 3 equal segments. One segment was dedicated to histological analysis, and the 2 other segments were kept in DMEM for 24 hours. Supernatant was collected, and proteins or total RNA were extracted from the arterial segments using Mammalian Cell Lysis Kit (Sigma-Aldrich, Saint-Quentin Fallavier, France) or Qiagen RNeasy extraction kit (Qiagen, Courtaboeuf, France) for biochemical and molecular biology analysis, respectively.

Histomorphometry and Immunochemistry Analysis

Carotid artery segments were cut and embedded in paraffin. Transversal sections were stained with orcein and van Gieson to visualize elastin and Sirius Red to visualize collagen. Autofluorescence of elastin fibers was also evaluated using fluorescence microscopy. Lumen, intima plus media, and total areas were measured in seeded and unseeded arteries (IPS 4.02 software, Tribvn, Chatillon, France). Elastin and collagen densities were quantified in the media, as previously described.[16] Briefly, sections were stained with orcein to evaluate elastin, which appeared in purple. Quantification of elastin density in the media was performed in 4 segments of each artery using dedicating software (IPS 4.02 software). Histological quantification of elastin was performed in 3 steps. First, the color image was transformed into monochrome with a 255-level gray scale. Thereafter, we evaluated the relative number of pixels classified as purple in the media by adjusting the threshold permitting a binary analysis. Similarly, we quantified the total pixels in the media. Elastin density was computed by the area of the pixels classified as elastin in the media divided by the area of total pixels in the media. Sections were stained with Sirius Red to evaluate collagen density. Collagen density was quantified the same way as elastin density. A semiquantitative grading of elastin was also performed as follows: (1) indicating no elastin visualization, (2) severely fragmented and disorganized elastin fibers, (3) moderately fragmented and disorganized elastin fibers, (4) normal elastin network with wavy elastic fibers and persistent fragmentation, and (5) normal elastin network with wavy elastic fibers and without fragmentation.

MMP-9 and TIMP-1 were detected using a monoclonal mouse anti-rabbit MMP-9 antibody (Abcam, Paris, France) and monoclonal mouse anti-rabbit TIMP-1 antibody (R&D systems, Lille, France). Inflammatory cells were detected with a monoclonal mouse anti-human CD45 antibody (AbCys, Paris, France). Human GF seeded in the arterial wall and in cell culture were detected by immunofluorescence using a monoclonal mouse anti-human lamin A/C antibody (Santa Cruz Biotechnology, Santa Cruz, CA) and a monoclonal mouse anti-human human leukocyte antigen-ABC antibody (BioLegend, San Diego, CA). VSMC were simultaneously detected on tissue sections separated by 7 μm using a monoclonal mouse anti–alpha smooth muscle actin (Sigma-Aldrich) to evaluate localization of human GF and VSMC 3, 7, and 21 days after cell therapy. Sections not treated with primary antibody were used as negative controls.

MMP, TIMP, and Cytokines Secretion Analysis

MMP-2 and MMP-9 activities were analyzed both in the supernatant and tissue extract of artery segments cultured during 24 hours using gelatin zymography, as previously described.[14,15,17] ELISA kits were also used to measure Pro-MMP-1, MMP-2, MMP-3, MMP-9, TIMP-1, transforming growth factor-β1 (TGF-β1), interleukin-1β (IL-1β), IL-4, IL-6, MMP-1/TIMP-1, MMP-3/TIMP-1, MMP-9/TIMP-1, and MMP-2/TIMP-2 complexes (all from R&D Systems).[14]

TIMP-1 secretion analysis by ELISA was performed using an antibody which cross-reacts with human and rabbit TIMP-1. Additional experiments were performed using a specific antibody of human TIMP-1 (DY970, R&D Systems). TIMP-1 was also analyzed by Western blotting and quantitative real-time polymerase chain reaction (see File II in the online-only Data Supplement).

Ex Vivo Rabbit and Human Aorta and GF Cocultures

Calibrated sections (4 mm) from normal rabbit abdominal aorta were embedded in a 10-mL mixture of 2-mg/mL collagen (Jacques Boy, Reims, France), 10% fetal bovine serum DMEM, and 0.1-M NaOH, and cultivated in 4 experimental conditions. Aorta segments were cocultured with rabbit GF only, rabbit GF and TIMP-1 blocking peptides (Tebu-Bio, Le Perray en Yvelines, France), TIMP-1 (100 ng/mL), or DMEM (control). Proteins extracted from aorta segments and supernatant were collected 1, 2, or 3 weeks after aorta embedding, as previously described.[14] MMP-9 and TIMP-1 proteins were quantified by ELISA. In each group, rabbit abdominal aorta segments were also dedicated for histology and stained with orcein to evaluate the elastin network.

Calibrated explants (4 mm) from AAA samples collected by surgery (n=6) were similarly embedded in collagen and cultivated with either human GF or DMEM (control) for 7 days. Protein extract and supernatant were collected before and 7 days after coculture with GF or DMEM. All samples were obtained with informed consent.

Viability Analysis Using Cell Culture

Carotid aneurisms in vivo seeded with human GF were harvested 1, 2, and 3 weeks after cell transplantation (n=3 for each time point). Aneurism explants were used as a source of primary culture. Calibrated explants (2 mm) from aneurismal samples were cultured with DMEM 20% fetal bovine serum. Cells growing out of the explants were retrieved 4 days later after trypsin digestion, seeded in labtek, and incubated for 24 hours at 37°C in DMEM 10% fetal bovine serum. Cells were then fixed with alcohol for 10 minutes and stored in PBS at 4°C for immunochemistry analysis.

Human Lamin A/C mRNA Relative Quantification

Total RNA from rabbit carotid aneurisms was extracted 3, 7, 14, and 21 days after human GF injection using Qiagen RNeasy extraction fibrous tissue (Qiagen). The quantitative measurement of total RNA and human lamin A/C mRNA was performed by real-time polymerase chain reaction (for details, see File II in the online-only Data Supplement).

Statistical Analysis

The primary end point of the study was the reduction of carotid diameter 1 month after seeding. We calculated that a sample size of 12 rabbits per group would allow us to detect a difference of 1.0 mm in the mean external diameter of the carotid arteries in the 2 experimental groups with a power of 80% and α of 0.05 using a 2-sided Mann-Whitney test.

Data are expressed as mean±SD. Comparison between arteries seeded with fibroblasts (GF- or DF-treated arteries) and a control solution (DMEM-treated arteries) is made by a Mann-Whitney test. A nonparametric ANOVA (Kruskal-Wallis) test was used to compare delta threshold cycle values in GF-treated arteries 3, 7, 14, and 21 days after cell therapy. Values were considered statistically different when P was <0.05.

Results

Regression of Carotid Aneurism by GF Therapy

One month after cell therapy, external carotid diameter significantly decreased in GF-treated arteries compared with DMEM-treated arteries (Figure 1A). There was a 23.3% carotid diameter reduction in GF-treated arteries and a 12% carotid diameter increase in DMEM-treated arteries 1 month after treatment (P<0.001). External carotid diameter still increased in DMEM-treated arteries in 3 months (+21.9%, Figure 1A). In contrast, carotid diameter in GF-treated arteries was stabilized in 3 months (−17.6%, Figure 1A).

Histomorphometric analysis confirmed the favorable effect of GF on carotid aneurism reduction, 1 and 3 months after cell therapy (Figure 1B). There was a significant reduction of total arterial area in GF-treated arteries compared with DMEM-treated arteries (−41.2% and −51.1%, 1 and 3 months after cell therapy, respectively; Figure 1B). There was also a significant reduction of luminal area in GF-treated arteries compared with DMEM-treated arteries, 3 months after cell therapy (Figure 1B). In DMEM-treated arteries, total arterial area increased by +30.4% from 1 to 3 months (Figure 1B). DF did not reduce the size of carotid aneurysms (File IIIA and IIIB in the online-only Data Supplement).

Impact of GF Therapy on Inflammatory Reaction

In DMEM-treated arteries, CD45$^+$ cells were present in the arterial wall and detected in 3 layers (Figure 2A). In GF-treated arteries, CD45$^+$ cells were reduced compared with the DMEM-treated arteries, 1 and 3 months after cell therapy (Figure 2A).

IL-4 and TGF-β1 levels in the supernatant and in the tissue extracts in GF-treated arteries were significantly higher than in DMEM-treated arteries (Figure 2B and 2C). IL-1β and IL-6 were significantly lower in GF-treated arteries than in DMEM-treated arteries in the supernatant and the tissue extracts (Figure 2D and 2E).

Extracellular Matrix Changes Associated With GF Therapy

We did not observe significant difference in collagen density between GF- and DMEM-treated arteries, 1 and 3 months after therapy (data not shown).

The elastic network was severely disorganized in DMEM-treated arteries in 1 and 3 months and presented with disruption of elastic lamellae. Elastin fibers, including internal and external elastic lamina, were either shortened or absent. Disrupted elastic lamellae exhibited flattened morphology instead of the wavy morphology observed usually in normal carotid arteries, (Figure 3A and 3C; File IV in the online-only Data Supplement). The media elastin density was significantly decreased in DMEM-treated arteries compared with normal arteries (Figure 3B). In contrast, in GF-treated arteries, we observed regeneration of the external and internal elastic lamina, as well as continuous

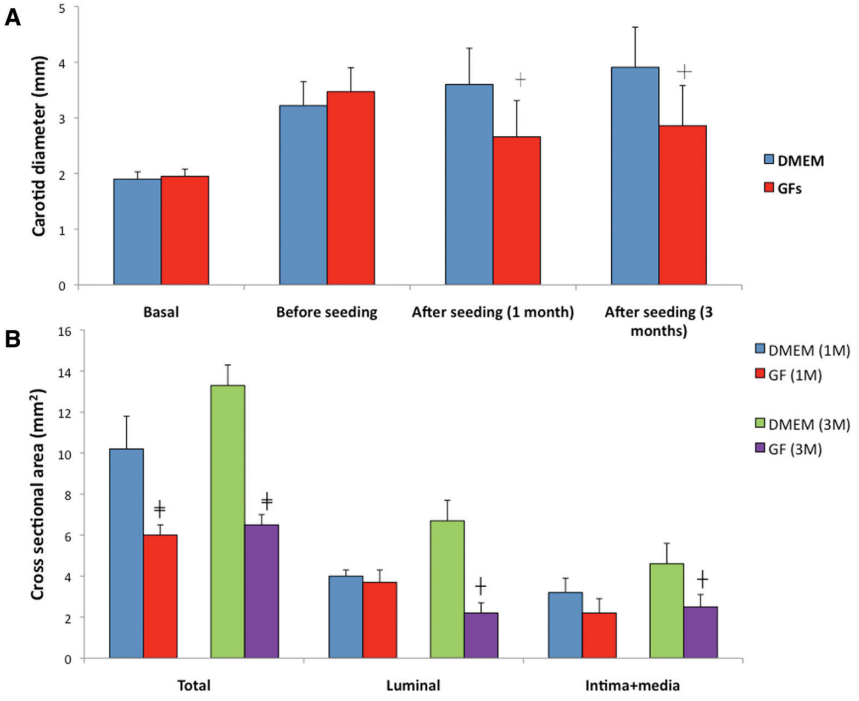

Figure 1. Reduction of carotid aneurism by gingival fibroblast (GF). **A,** Bar graph representation of external carotid diameters at baseline, before, and 1 and 3 months after seeding in arteries treated with a control solution (DMEM; blue; n=23) or with GF (red; n=23). **B,** Bar graph representation of histomorphometric quantification of total, luminal, and intima+media cross-sectional areas in GF- (n=23) and DMEM- (n=23) treated arteries, 1 and 3 months after treatment (blue: DMEM in 1 month; green: DMEM in 3 months; red: GF in 1 month; and purple: GF in 3 months). *P<0.05, †P≤0.01, ‡P≤0.001.

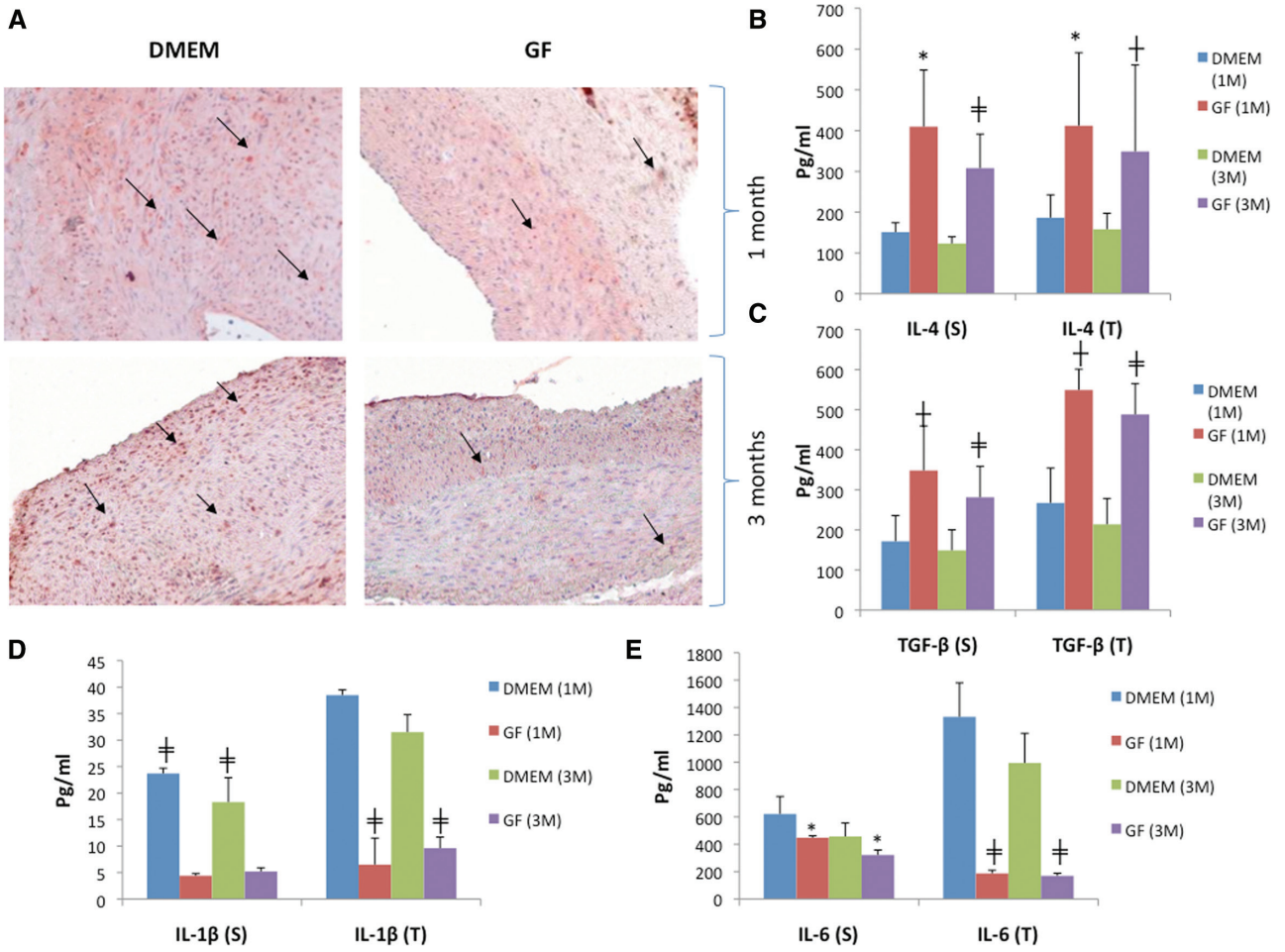

Figure 2. Impact of gingival fibroblast (GF) on inflammation. **A,** Immunostaining with anti-CD45 antibody to detect inflammatory cells in DMEM- and GF-treated arteries, 1 and 3 months after seeding. Positive staining appears red in the 3 layers of the arteries. Sections were counterstained with hematoxylin. Magnification, ×20. **B** to **E,** Bar graph representation of the concentration of interleukin-4 (IL-4, **B**), transforming growth factor-β1 (TGF-β1, **C**), IL-1β (**D**), and IL-6 (**E**) measured by ELISA in the supernatant (S) and the tissue (T) of DMEM- (blue and green; n=23) or GF- (red and purple; n=23) treated arteries, 1 and 3 months after treatment. *P<0.05, †P≤0.01, ‡P≤0.001.

and wavy elastic fibers although thinner than in normal arteries (Figure 3A and 3C; File IV in the online-only Data Supplement). This structural reorganization resulted in a significant increase in elastin density in GF-treated arteries compared with DMEM-treated arteries, 1 and 3 months after cell therapy (38.2±8.4% versus 18.0±5.8%; P=0.016; Figure 3B). Arteries treated with GF had a semiquantitative grading score significantly higher than those treated with culture medium (DMEM; 3.1±0.4 versus 1.9±0.7; P<0.05). In contrast, elastin remained altered after DF infusion (File IIIC in the online-only Data Supplement).

Impact of GF Cell Therapy on MMP-9 and TIMP-1

In DMEM-treated arteries, MMP-9 immunostaining was detected in all the layers of the artery in 1 and 3 months whereas TIMP-1 immunostaining was faint or absent (Figure 4A and 4B). In contrast, in GF-treated arteries, MMP-9 immunostaining was barely present whereas TIMP-1 immunostaining was strongly detected, 1 and 3 months after cell therapy (Figure 4A and 4B).

MMP-9 activity (zymography) significantly decreased in GF-treated arteries, 1 and 3 months after cell therapy compared with DMEM-treated arteries (Figure 4C). In parallel, TIMP-1 significantly increased in GF-treated arteries compared with DMEM-treated arteries (Western blotting analysis; Figure 4D). Raw data of Western blotting analysis are shown in File V in the online-only Data Supplement.

These results were confirmed by ELISA analysis. MMP-9 protein content was significantly decreased in GF-treated arteries compared with DMEM-treated arteries as soon as 3 days (0.50±0.68 versus 1.58±0.20 ng/mL; P<0.05) but also 1 and 3 months after cell therapy (Figure 4E). There was a significant increase of TIMP-1 content in GF-treated arteries compared with DMEM-treated arteries, 1 and 3 months after cell therapy. Using a specific antibody against human TIMP-1, we demonstrated the contribution of GF as soon as 3 days after cell therapy (0.30±0.03 ng/mL) because we did not detect human TIMP-1 either in DMEM-treated arteries or in control normal arteries. Increase of TIMP-1 protein release (Figure 4D) corresponded with an increase of TIMP-1 mRNA expression (File VIA in the online-only Data Supplement). There was a significant 2.5-fold increase in MMP-9/TIMP-1 complex formation in GF-treated arteries (Figure 4E). Similar observations were obtained from the

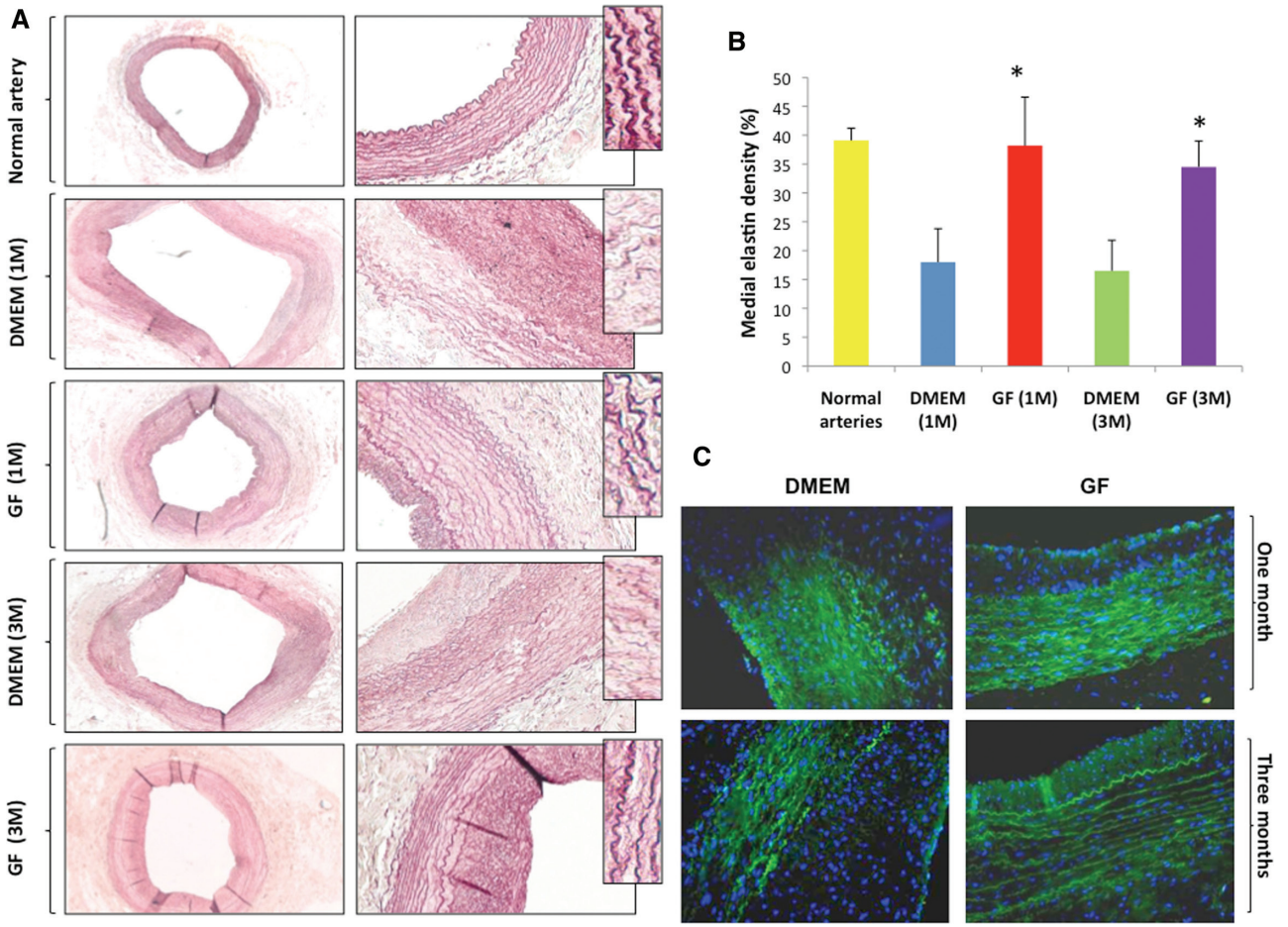

Figure 3. Gingival fibroblast (GF) reduced carotid aneurism and resulted in elastin network repair. **A,** In vivo visualization of elastin network in normal, DMEM-, and GF-treated rabbit carotid arteries, 1 and 3 months after treatment. Magnification, ×5 (left column) and ×20 (right column). **B,** Bar graph representation of elastin density in the media of normal arteries (yellow; n=6), in DMEM- (blue and green; n=23) or GF- (red and purple; n=23) treated arteries, 1 and 3 months after treatment. *P<0.05. **C,** Autofluorescence of elastin network in GF- or DMEM-treated arteries, 1 and 3 months after treatment. Nuclei were labeled in blue using 4',6-diamidino-2-phenylindole (DAPI).

supernatant collected 24 hours after incubation of calibrated artery segments.

Other MMPs and corresponding TIMPs measurements were also performed and are shown in File VIB in the online-only Data Supplement. Pro–MMP-1 and MMP-3 levels were lower in GF-treated arteries, and the levels of corresponding MMP/TIMP-1 complexes were higher than in DMEM-treated arteries.

In an ex vivo rabbit aorta model MMP-9 activity spontaneously increased, and elastin network was fragmented in cultured rabbit aorta alone and preserved in incubated segments with either GF or TIMP-1 (Figure 5A–5F). MMP-9 concentration was decreased in the presence of GF or TIMP-1 (Figure 5F). Incubation of rabbit aorta segments with GF and a TIMP-1 blocking peptide abolished the favorable effect of GF on elastin network preservation and on the inhibition of MMP-9 level (Figure 5D–5F). TIMP-1 level was still increased, because of GF presence, confirming that the peptide only blocked TIMP-1 activity (Figure 5F). DFs did not show significant variation of MMP-9, TIMP-1, and cytokines (File IIID in the online-only Data Supplement).

In Situ Detection and Viability of GF After Cell Transplantation

Human lamin A/C-positive cells were abundantly detected in human GF-treated arteries in the media and adventitia up to 14 days after seeding, suggesting that they could play a role in repairing medial structure (Figure 6A; File VII in the online-only Data Supplement). From day 21 until 3 months, GF were mainly detected in the adventitia. GF did not colocalize with VSMC. This was confirmed by relative quantitative real-time polymerase chain reaction analysis of human lamin A/C mRNA in presence of GF. Real-time polymerase chain reaction specificity was testified by the 107-bp amplicon length corresponding to human lamin A/C expression (Figure 6B and 6C). This expression was high and stable over time, as shown in Figure 6C.

Human mRNA analysis supported that in vivo seeded human GF were viable in the treated aneurismal rabbit arteries. This was reinforced by the analysis of cells harvested 1, 2, and 3 weeks after human GF transplantation, which were able to grow out of the arteries, and were abundantly present (Figure 6D). At all time points of tissue collection, cells present in the cultures had typical shape of GF, and the majority positively

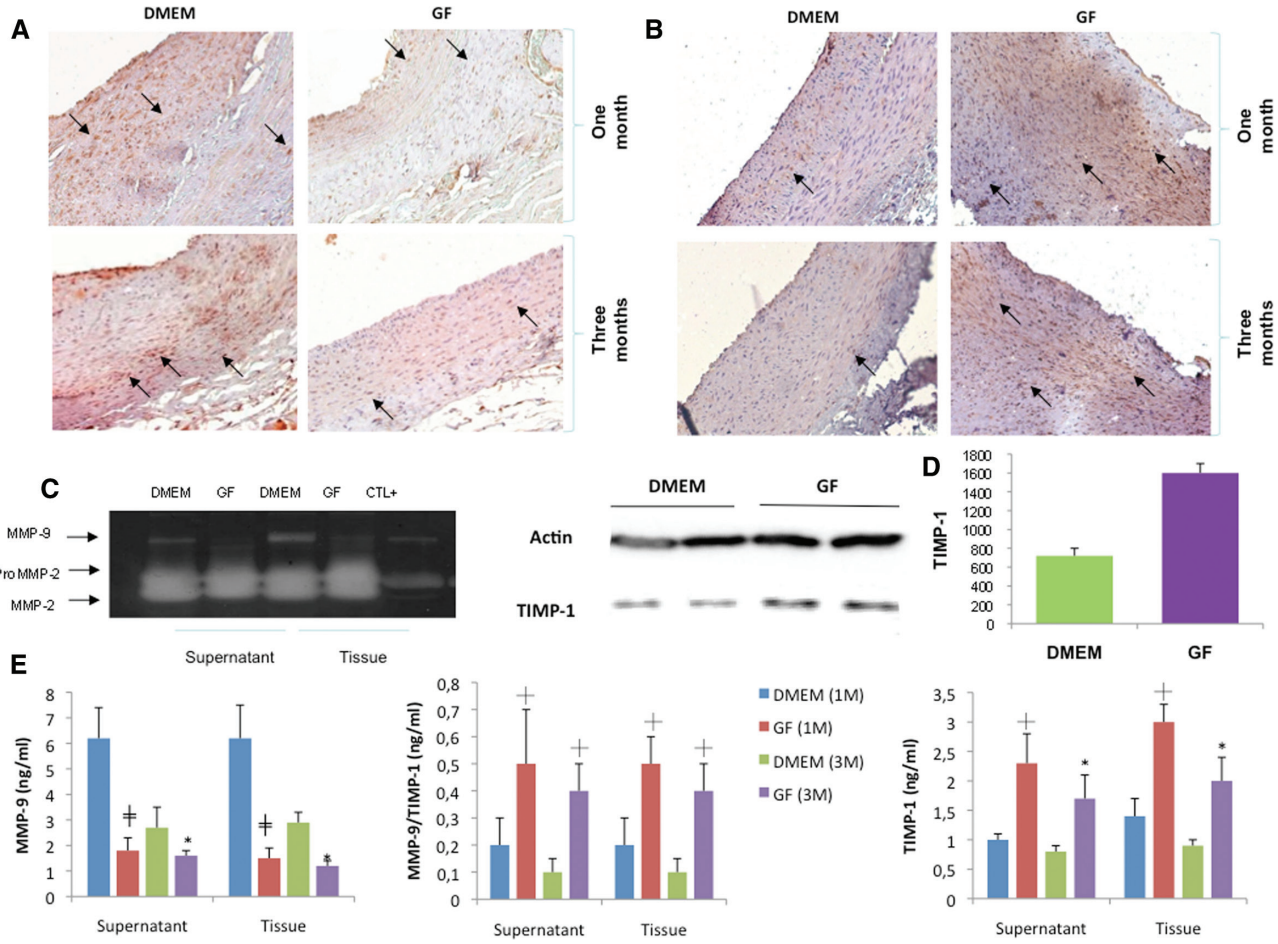

Figure 4. Impact of gingival fibroblast (GF) on matrix metalloproteinase-9 (MMP-9) and tissue inhibitor of metalloproteinase 1 (TIMP-1). **A** and **B,** Immunostaining with an antibody against MMP-9 (**A**) and TIMP-1 (**B**) in DMEM- and GF-treated arteries, 1 and 3 months after treatment. Sections were counterstained with hematoxylin. **C,** Zymography analysis of MMP-2 and MMP-9 in DMEM- and GF-treated arteries in the tissue extract and supernatant. **D,** Bar graph representation and Western blotting analysis of TIMP-1 in DMEM- (n=2) and GF-(n=2) treated arteries, 3 months after treatment. **E,** Bar graph representation of the concentration of MMP-9, TIMP-1, and MMP-9/TIMP-1 complexes measured by ELISA in the supernatant and the tissue extract of DMEM- (blue and green; n=23) or GF- (red and purple; n=23) treated arteries, 1 and 3 months after treatment. **P*<0.05, †*P*≤0.01, ‡*P*≤0.001. Magnification, ×20. Sections were counterstained with hematoxylin (**A** and **B**).

stained with human lamin A/C and human leukocyte antigen antibodies, confirming their human gingival origin.

Relevance of GF Therapy for Human AAA Treatment

Ex vivo MMP-9 activity of human pathological samples decreased with or without GF on day 7 compared with day 0 (Figure 7A and 7B). However, we observed on day 7 that MMP-9 activity and secretion was significantly lower in AAA cultured with GF than in those with culture medium. In the presence of GF, MMP-9 activity was barely detectable (Figure 7A). ELISA analysis confirmed the decrease of MMP-9 secretion (Figure 7B). MMP-9 activity reduction was associated with a 3-fold increase of its inhibitor TIMP-1 and the formation of MMP-9/TIMP-1 complexes (Figure 7C and 7D).

Discussion

The present study tested the following hypothesis: can we use the healing potential of a tissue with embryo-like repair ability (ie, gum) to improve the healing of another organ (ie, artery) from the same human adult? Indeed, among organs in humans, the capacity of healing is highly variable: from almost none in brain to very high in gum.[18]

We demonstrated that in vivo transient endoluminal contact between GF suspension and the aneurismal arterial wall resulted not only in stabilization of the aneurism but also in its regression, 1 month after cell therapy and the persistence of the effects after 3 months, in contrast with previous studies using other cell types or gene therapy.[7–11] This benefit was illustrated by the reduction of expansive remodeling, which was associated not only with reduction of elastolysis but also with restoration of the elastin network. To our knowledge, this is the first time that elastin repair has been observed, and it is related not only to stabilization but also to reduction of aneurism formation. In a rat model of aneurismal aortic xenografts, VSMC therapy resulted in aortic diameter stabilization and elastolysis reduction.[11]

GF-mediated elastin repair was related to a decrease of elastin degradation or an increase of elastin synthesis. In our study, in situ elastolysis was dramatically decreased, as a

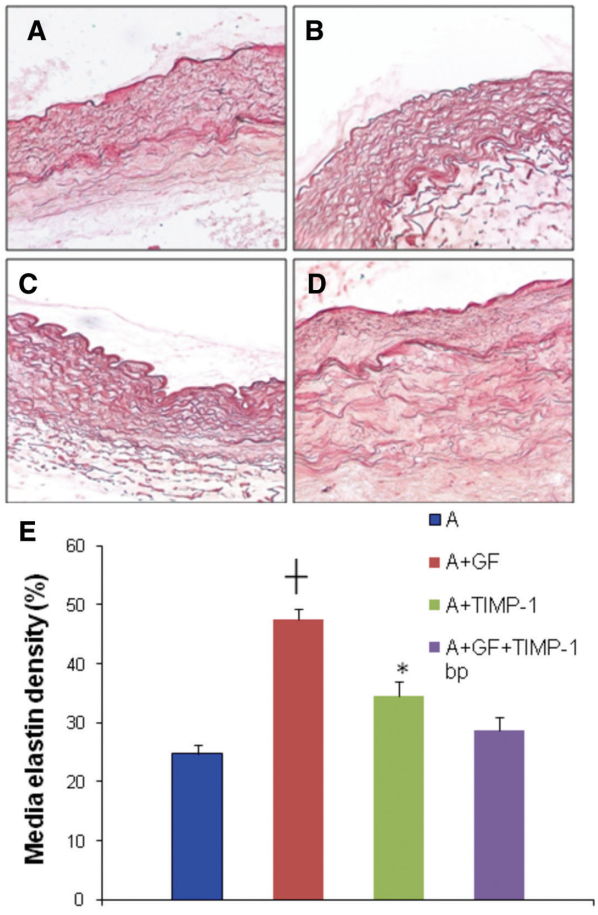

F

		TIMP-1 (ng/ml)	MMP-9 (ng/ml)
7 DAYS	A	1.17 ± 0	1.48 ± 0.08
	A + GF	1.3 ± 0.1	0.5 ± 0.04
	A + TIMP-1	2.57 ± 0.06	1.32 ± 0.1
	A + GF + TIMP-1 bp	1.69 ± 0.06	1.24 ± 0.06
14 DAYS	A	ND	2.37 ± 0.06
	A + GF	2.8 ± 0.04	1.15 ± 0.05
	A + TIMP-1	3.16 ± 0.19	2.01 ± 0.08
	A + GF + TIMP-1 bp	3.32 ± 0.17	1.45 ± 0.05
21 DAYS	A	ND	2.69 ± 0.02
	A + GF	3.26 ± 0.0	0.98 ± 0.04
	A + TIMP-1	2.08 ± 0.04	2.17 ± 0.02
	A + GF + TIMP-1 bp	2.23 ± 0.0	1.06 ± 0.03

Figure 5. Inhibition of elastin network gingival fibroblast (GF)–induced repair by tissue inhibitor of metalloproteinase 1 (TIMP-1) blocking peptide. **A** to **D,** Elastin network in an ex vivo rabbit aorta model alone (**A**; n=3), in coculture with GF (**B**; n=3), in presence of TIMP-1 (**C**; n=3), and in coculture with GF and a TIMP-1 blocking peptide (**D**, n=3) after 21 days in culture. Sections were stained with orcein. Magnification, ×20. **E,** Bar graph representation of elastin density (21 days) in the media of aorta alone (blue), aorta+GF (red), aorta+TIMP-1 (green), and aorta+GF+TIMP-1 blocking peptide (TIMP-1 bp, purple). *P<0.05, †P≤0.01. **F,** Matrix metalloproteinase-9 (MMP-9) and TIMP-1 analysis by ELISA in the supernatant on 7, 14, and 21 days after ex vivo coculture of aorta (**A**) and GF, aorta and TIMP-1, aorta+GF+TIMP-1 blocking peptide (bp), or aorta alone.

result of MMP-9 inactivation by TIMP-1 stimulation. Ex vivo experiments clearly demonstrated that GF reduced elastolysis through TIMP-1 overexpression because incubation of rabbit aorta segments with GF and a TIMP-1 blocking peptide abolished the favorable effect of GF on elastin network preservation. These data confirmed our observation made in vitro using a model of spontaneous degradation of elastin in rabbit abdominal aorta segments[14] and provided evidence that TIMP-1 is a key factor in the protection offered by GF also in vivo. There are 2 potential sources of cells surexpressing TIMP-1 in the present study: resident VSMC and GF. Using human GF in aneurismal rabbit carotid arteries and specific antibody of human TIMP-1 for ELISA analysis which does not cross-react with rabbit TIMP-1, we demonstrated that GFs contribute to TIMP-1 surexpression as soon as 3 days after cell therapy until the end of the study follow-up (3 months). A stimulation of TIMP-1 secretion by VSMC cannot be excluded, contributing also to the decrease in MMP-9 activity. This has been previously reported by our group using in vitro models.[14] Moreover, GF reduced in vivo inflammatory cell accumulation and inflammatory cytokine expression also contributing to alterations in the proteolytic environment because inflammatory cells produce large amount of MMP-9.

On the other hand, GF may also increase elastin synthesis. Elastin synthesis is mediated by resident adventitial fibroblast and VSMC in the arterial wall. First, one can hypothesize that transplanted GFs are a potential direct source of elastin repair because it has been previously reported that GF produced microfibrils and elastin.[19] Second, an indirect effect of GF is also possible. GF may interact with resident VSMC and adventitial fibroblasts and increase elastin synthesis from these cells. In particular, it has been previously reported that TGF-β1 stimulates elastin synthesis,[20] and interestingly we observed that GF increase the production of TGF-β1 both in vitro and in vivo. Finally, reduction of smooth muscle apoptosis may also contribute to increased elastin density, although additional mechanisms could not be excluded.

We evaluated the safety, persistence, and viability of GF up to 3 months after cell therapy. We showed that endoluminal infusion of rabbit or even human GF into aneurismal rabbit carotid arteries was feasible and safe without adverse events. Inflammation plays an important role in the pathogenesis of AAA.[2,5] Interestingly, GF transplantation was not associated with increased inflammatory reaction. In contrast, although presence of inflammatory cells was observed in the arterial wall of control aneurismal carotids, we found a significant reduction of $CD45^+$ cells after GF cell therapy. Furthermore, GF cell therapy was associated with reduction in proinflammatory cytokines (IL-1, IL-6) and an anti-inflammatory cytokine increase (TGF-β1 and IL-4). This modulation of inflammatory markers may explain the reduction of neointima+media observed in GF-treated arteries. We demonstrated that GF penetrated the arterial wall, and remained detectable, 3 months after cell therapy in all transfected arteries, although a limited proportion of GF was detected in 1 and 3 months. These cells were viable because we were able to culture human GF harvested from aneurismal carotid arteries. In the setting of cell therapy using bone marrow–derived multipotent progenitor

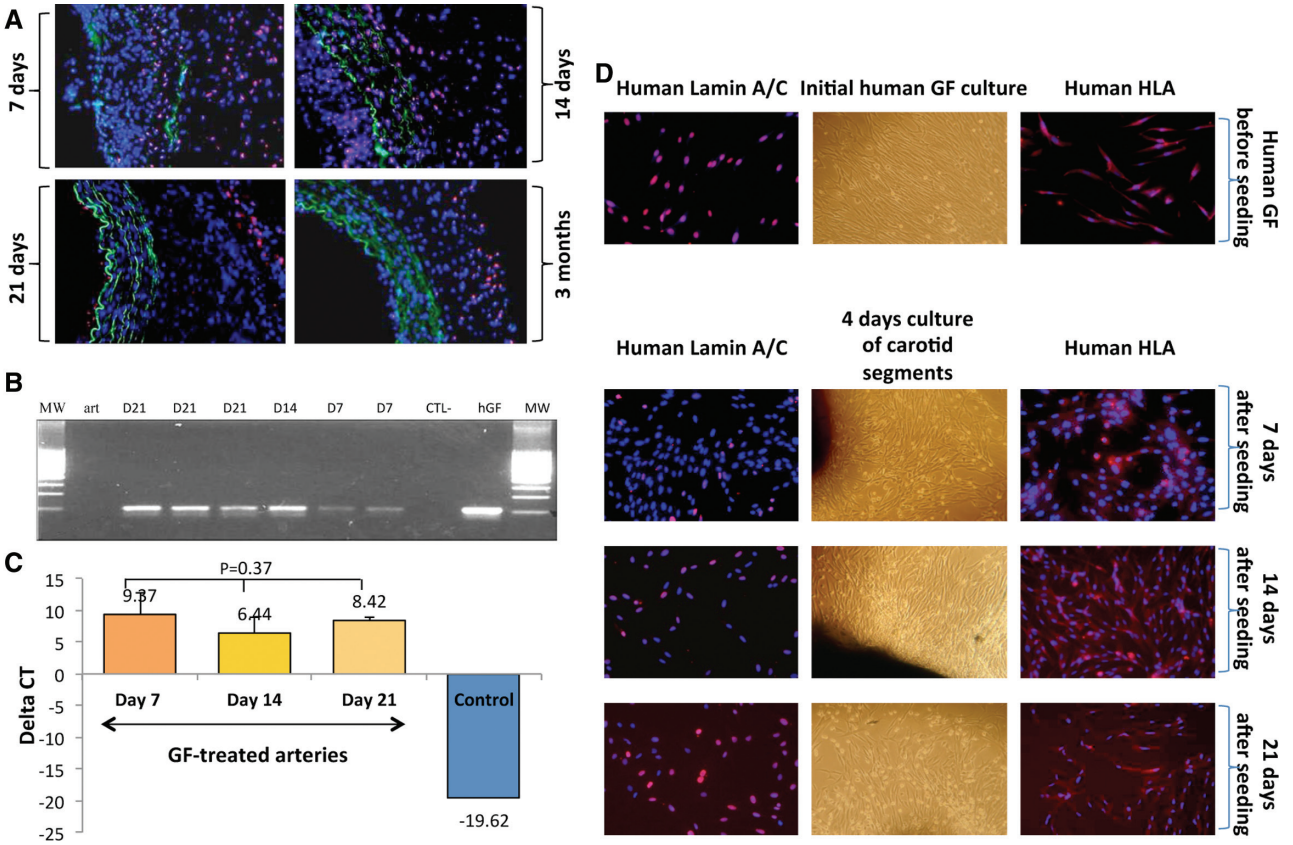

Figure 6. Localization, characterization, and viability of gingival fibroblast (GF). **A,** Immunostainings using a monoclonal mouse anti-human lamin A/C antibody to detect human GF seeded into the arterial wall (n=12). Sections were counterstained with 4',6-diamidino-2-phenylindole (DAPI; blue), and autofluorescence elastin fibers appeared in green. Magnification, ×20. **B,** Migration in a 2% agarose gel of mRNA extracted from rabbit arteries amplified with specific human lamin A/C primer. A specific 107-bp band corresponding to human lamin A/C was present in human GF seeded arteries on 7, 14, and 21 days but absent in DMEM-treated rabbit arteries. **C,** Bar graph representation of relative mRNA expression of human lamin A/C. Delta threshold cycle (ΔCT) analysis showed that the expression of human lamin A/C was persistent and stable 7, 14, and 21 days after seeding with human GF. **D,** Phase contrast analysis and immunostainings with monoclonal mouse anti-human lamin A/C and human leukocyte antigen (HLA) antibodies (red stainings), counterstained with DAPI (blue staining). In the initial human GF culture (before grafting in rabbit aorta), all the cells presented the shape of human GF, and were positive for both human lamin A/C and HLA. An abundant cell outgrowth was observed after 4 days in culture of the rabbit carotid aneurism segments harvested 7 (n=3), 14 (n=3), and 21 (n=3) days after in vivo treatment by human GF. Numerous human lamin A/C and HLA-positive cells were detected (red stainings) 7 to 21 days after seeding, confirming the persistence of viable GF in the artery wall. For these experiments, human GF were used.

cells in the early phase of postmyocardial infarction, a very low rate of sustained cell engraftment was observed regardless of the route of cell transfer.[21] More than 90% of injected cells disappeared over the first days, and <1% of donor cells could still be identified 4 weeks after transplantation.[22] This low rate of engraftment may be linked to early cell death or apoptosis related to the biological process that occurs before incorporation of the cells into the myocardium, and to the late death of cells initially retained, secondary to inflammation.[23]

In our study, cell therapy using GF was associated with a persistent reduction of carotid aneurism in 3 months whereas control carotid aneurisms continued to progress. Interestingly, inhibition of MMP-9 via TIMP-1 overexpression also persisted in 3-month follow-up. These results indicate that endoluminal GF cell therapy is a promising new strategy, avoiding pretreatment with gene therapy, and the cells are easy to collect with the ability to grow in culture compared with VSMC or stem cells. Moreover, human GF exhibited both ex vivo in human AAA sample cocultures, and in vivo in the rabbit, their ability to appropriately increase TIMP-1, and to restore elastic network.

DF did neither reduce aneurism nor restore the elastin network, confirming that aneurism reduction and restoration of the elastin network is GF-specific, most likely resulting from TIMP-1 overexpression. The issue of cell specificity also concerns the specificity of the target artery. GF interact only with diseased vessels: GF have no effect on normal arteries (Durand E, Fournier B, Couty L, Coulomb B, Lafont A, unpublished data, 2011). The beneficial effects of GF may therefore relate to their capacity to interact with the local pathological arterial environment: through the transmembrane-anchoring integrins, GF may perceive the presence and the structure of surrounding macromolecule alterations as in gingival.[18]

Our ex vivo coculture experiments of GF and human AAA samples demonstrated that GF decreased MMP-9 via TIMP-1 overexpression also in pathological human tissues. Furthermore, the short period of in situ incubation (15 minutes) of GF seeding in the rabbit arterial wall may be clinically adaptable for the

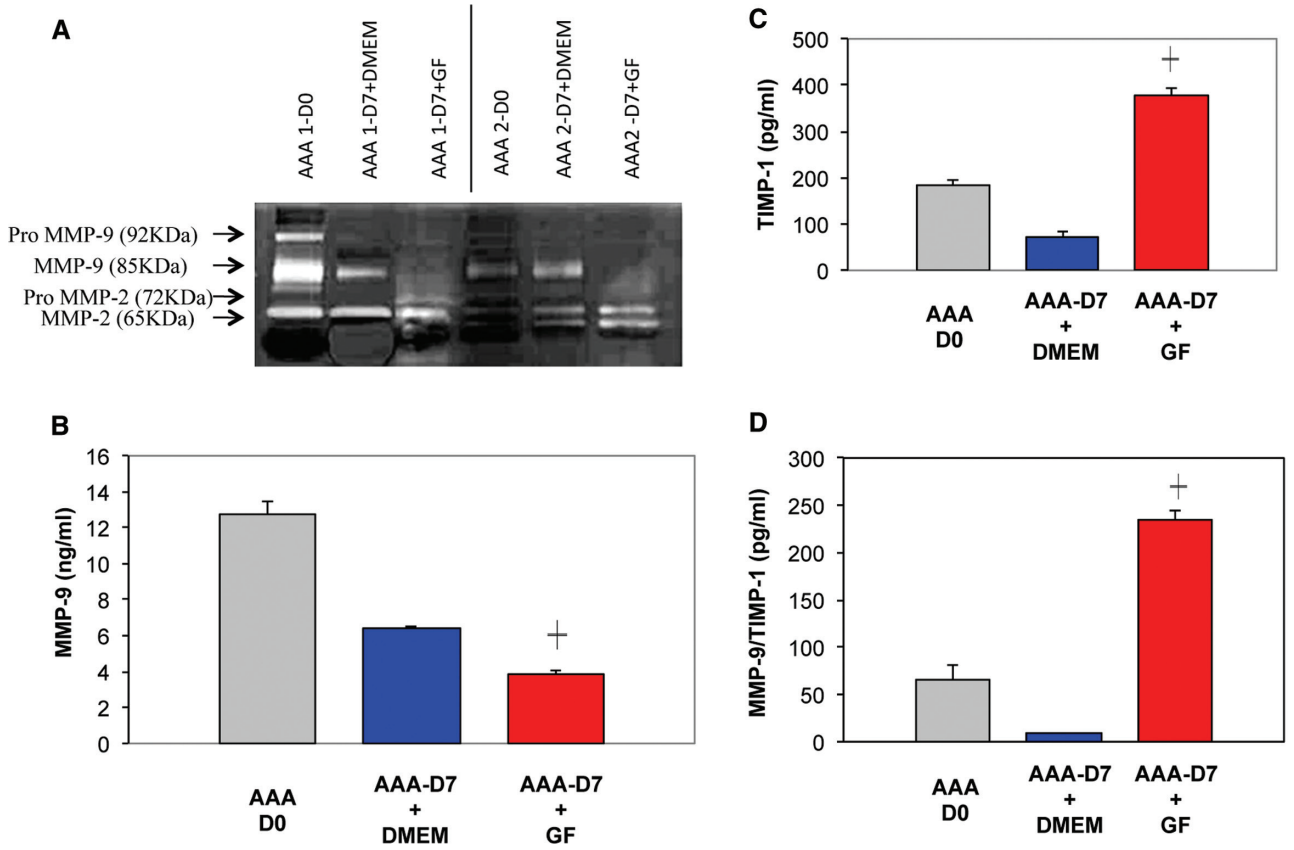

Figure 7. Efficacy of gingival fibroblast (GF) in human abdominal aortic aneurism. **A,** Zymography analysis of matrix metalloproteinase-2 (MMP-2) and MMP-9 in human abdominal aortic aneurism (AAA; n=6) samples 7 days after ex vivo treatment either with DMEM or GF. MMP-9 activities were decreased in AAA treated with GF compared with those with DMEM. **B** to **D,** Bar graph representation of concentration of MMP-9 (**B**), tissue inhibitor of metalloproteinase 1 (TIMP-1; **C**), and MMP-9/TIMP-1 complexes (**D**) measured by ELISA in tissue extracts of human AAA (n=6) cocultured with or without GF. ‡$P \leq 0.001$. For these experiments, human GF were used.

treatment of AAA in humans. We believe that our study represents a step toward potential clinical applications. Endovascular approach assisted with a specific cell therapy could allow the treatment of earlier stages of aneurismal disease.

Our results were obtained in vivo using a rabbit model of elastase-induced aneurisms. Extrapolation to the more complex human AAA disease requires caution, although we tested the efficacy of human GF on human AAA samples ex vivo.

In conclusion, our study aimed to validate the concept of cell therapy using GF to restore the elastic network and reduce arterial aneurism via TIMP-1 overexpression. Autologous GF cell therapy appears as a novel strategy. Cells are easy to collect and to seed in the artery wall with persistence and viability of GF, resulting in aneurism reduction. Further studies are warranted to validate the percutaneous approach to be clinically adaptable for the treatment of AAA in humans.

Acknowledgments

We thank Julie Piquet for technical assistance during animal experiments and Annie Herbert for reviewing the article.

Sources of Funding

This study was supported by a grant from INSERM, Université Paris Descartes, Paris, France and Agence Nationale de la Recherche (ANR, 07-EMPB-027-01).

Disclosures

B. Gogly, B. Coulomb, and A. Lafont are cofounders of the startup Scarcell Therapeutics. The other authors have no conflicts to report.

References

1. Sakalihasan N, Limet R, Defawe OD. Abdominal aortic aneurysm. *Lancet*. 2005;365:1577–1589.
2. Shah PK. Inflammation, metalloproteinases, and increased proteolysis: an emerging pathophysiological paradigm in aortic aneurysm. *Circulation*. 1997;96:2115–2117.
3. López-Candales A, Holmes DR, Liao S, Scott MJ, Wickline SA, Thompson RW. Decreased vascular smooth muscle cell density in medial degeneration of human abdominal aortic aneurysms. *Am J Pathol*. 1997;150:993–1007.
4. Longo GM, Xiong W, Greiner TC, Zhao Y, Fiotti N, Baxter BT. Matrix metalloproteinases 2 and 9 work in concert to produce aortic aneurysms. *J Clin Invest*. 2002;110:625–632.
5. Freestone T, Turner RJ, Coady A, Higman DJ, Greenhalgh RM, Powell JT. Inflammation and matrix metalloproteinases in the enlarging abdominal aortic aneurysm. *Arterioscler Thromb Vasc Biol*. 1995;15:1145–1151.
6. Luttun A, Lutgens E, Manderveld A, Maris K, Collen D, Carmeliet P, Moons L. Loss of matrix metalloproteinase-9 or matrix metalloproteinase-12 protects apolipoprotein E-deficient mice against atherosclerotic media destruction but differentially affects plaque growth. *Circulation*. 2004;109:1408–1414.
7. Allaire E, Forough R, Clowes M, Starcher B, Clowes AW. Local overexpression of TIMP-1 prevents aortic aneurysm degeneration and rupture in a rat model. *J Clin Invest*. 1998;102:1413–1420.
8. Qian HS, Gu JM, Liu P, Kauser K, Halks-Miller M, Vergona R, Sullivan ME, Dole WP, Deng GG. Overexpression of PAI-1 prevents

the development of abdominal aortic aneurysm in mice. *Gene Ther*. 2008;15:224–232.
9. Dai J, Losy F, Guinault AM, Pages C, Anegon I, Desgranges P, Becquemin JP, Allaire E. Overexpression of transforming growth factor-beta1 stabilizes already-formed aortic aneurysms: a first approach to induction of functional healing by endovascular gene therapy. *Circulation*. 2005;112:1008–1015.
10. Pyo R, Lee JK, Shipley JM, Curci JA, Mao D, Ziporin SJ, Ennis TL, Shapiro SD, Senior RM, Thompson RW. Targeted gene disruption of matrix metalloproteinase-9 (gelatinase B) suppresses development of experimental abdominal aortic aneurysms. *J Clin Invest*. 2000;105:1641–1649.
11. Allaire E, Muscatelli-Groux B, Guinault AM, Pages C, Goussard A, Mandet C, Bruneval P, Méllière D, Becquemin JP. Vascular smooth muscle cell endovascular therapy stabilizes already developed aneurysms in a model of aortic injury elicited by inflammation and proteolysis. *Ann Surg*. 2004;239:417–427.
12. Schor SL, Ellis I, Irwin CR, Banyard J, Seneviratne K, Dolman C, Gilbert AD, Chisholm DM. Subpopulations of fetal-like gingival fibroblasts: characterisation and potential significance for wound healing and the progression of periodontal disease. *Oral Dis*. 1996;2:155–166.
13. Häkkinen L, Uitto VJ, Larjava H. Cell biology of gingival wound healing. *Periodontol 2000*. 2000;24:127–152.
14. Gogly B, Naveau A, Fournier B, Reinald N, Durand E, Brasselet C, Coulomb B, Lafont A. Preservation of rabbit aorta elastin from degradation by gingival fibroblasts in an ex vivo model. *Arterioscler Thromb Vasc Biol*. 2007;27:1984–1990.
15. Reinald N, Fournier B, Naveau A, Couty L, Lemitre M, Seguier S, Coulomb B, Gogly B, Lafont A, Durand E. Fusiform aneurysm model in rabbit carotid artery. *J Vasc Res*. 2010;47:61–68.
16. Lafont A, Durand E, Samuel JL, Besse B, Addad F, Lévy BI, Desnos M, Guérot C, Boulanger CM. Endothelial dysfunction and collagen accumulation: two independent factors for restenosis and constrictive remodeling after experimental angioplasty. *Circulation*. 1999;100:1109–1115.
17. Naveau A, Reinald N, Fournier B, Durand E, Lafont A, Coulomb B, Gogly B. Gingival fibroblasts inhibit MMP-1 and MMP-3 activities in an ex-vivo artery model. *Connect Tissue Res*. 2007;48:300–308.
18. Bartold PM, Narayanan AS. Molecular and cell biology of healthy and diseased periodontal tissues. *Periodontol 2000*. 2006;40:29–49.
19. Tsuruga E, Irie K, Sakakura Y, Yajima T. Expression of fibrillins and tropoelastin by human gingival and periodontal ligament fibroblasts in vitro. *J Periodont Res*. 2002;37:23–28.
20. Sauvage M, Hinglais N, Mandet C, Badier C, Deslandes F, Michel JB, Jacob MP. Localization of elastin mRNA and TGF-beta1 in rat aorta and caudal artery as a function of age. *Cell Tissue Res*. 1998;291:305–314.
21. Dimmeler S, Burchfield J, Zeiher AM. Cell-based therapy of myocardial infarction. *Arterioscler Thromb Vasc Biol*. 2008;28:208–216.
22. Zeng L, Hu Q, Wang X, Mansoor A, Lee J, Feygin J, Zhang G, Suntharalingam P, Boozer S, Mhashilkar A, Panetta CJ, Swingen C, Deans R, From AH, Bache RJ, Verfaillie CM, Zhang J. Bioenergetic and functional consequences of bone marrow-derived multipotent progenitor cell transplantation in hearts with postinfarction left ventricular remodeling. *Circulation*. 2007;115:1866–1875.
23. Menasche P. Cardiac cell therapy: lessons from clinical trials. *J Mol Cell Cardiol*. 2011;50:258–265.